Ultra hard x rays from krypton clusters heated by intense laser fields

R. C. Issac,[a] G. Vieux, B. Ersfeld, E. Brunetti, S. P. Jamison, J. Gallacher, D. Clark, and D. A. Jaroszynski
University of Strathclyde, Department of Physics, John Anderson Building, 107 Rottenrow, Glasgow G4 0NG, Scotland, United Kingdom

The interaction of ultrashort laser pulses with krypton clusters at intensity up to 1.3×10^{18} Wcm^{-2} has been investigated. Intense Kα and Kβ emission from krypton at 12.66 and 14.1 keV, respectively, has been observed using conventional solid state x-ray detectors. The measured x-ray spectra have broad bremsstrahlung continuum reaching to photon energies up to 45 keV, with evidence that approximately 10% of electrons that are heated to very high electron temperatures, which is consistent with a two-temperature electron distribution. This is ascribed to the presence of a hot electron population, similar to that found in laser–solid interactions. The highest laser energy to x-ray conversion efficiency observed is 9.2×10^{-7}, which is equivalent to 45 nJ x-ray pulse energy from the 12.66 keV krypton Kα transition. © *2004 American Institute of Physics.* [DOI: 10.1063/1.1755222]

I. INTRODUCTION

Laser-produced plasma from optically ionized gases and solid density matter has been widely explored over the last two decades as a potential source of x-ray and extreme ultraviolet radiation,[1,2] following the advent of the chirped pulse amplified (CPA) tabletop terawatt laser. Compared with gas-phase targets, x-ray sources derived from solid targets have superior x-ray yields in the hard x-ray spectral region. Rare gas clusters have recently been considered as replacements for solid targets[3–5] because they are debris-free and yet retain solid-like properties. To date, x rays emitted from K, L and M shell vacancies in ions have been observed from argon clusters,[6] and L and M shell emission has been observed from clusters with higher atomic numbers such as krypton[7] and xenon.[8] Despite thorough investigation of hard x-ray generation from clusters, the highest x-ray photon energy reported so far is 3.3 keV from H-like argon measured at an intensity of 10^{17} Wcm^{-2}.[6] Furthermore, the study of x-ray emission from the plasma produced by ultrashort laser pulses yields additional information on plasma formation and its dynamics.

Collisional processes play a major role in the plasma formation owing to high atomic density inside clusters. The solid-like density allows them to be rapidly heated to very high temperatures using femtosecond lasers,[4] which also makes them very useful sources of energetic particles. Highly energetic ions[9] and electrons[10–12] have been observed from laser heated clusters. Collisions between ions during Coulomb explosions of laser irradiated deuterium clusters lead to the production of neutrons.[13] Alexeev *et al.*[14] showed that macroscopic propagation effects can modify the interaction process under appropriate conditions through self-focusing. Even at moderate intensities of below $\sim 10^{15}$ Wcm^{-2}, the clustered gas acts like a positive lens leading to self-focusing. Investigations on the heat transport in high temperature laser produced cluster plasma media indicate that heat transport drives a fast ignition wave.[15] Properties of the cluster media as well as the incident laser parameters such as laser intensity,[16] pulse duration,[7,12,17,18] laser wavelength,[19] polarization,[8,20] presence of pre-pulse[21] and the residual chirp[18] play a vital role in optimizing particle and photon emission from rare gas clusters.

In this article, we report x-ray continuum and Kα (12.66 keV) emission from laser heated krypton clusters with optimum yields of 45 nJ/pulse, which gives an overall efficiency of $\sim 9.2 \times 10^{-7}$, the highest yet measured from rare gas clusters at this photon energy. The measured x-ray bremsstrahlung continuum is consistent with a two-temperature plasma that has been rapidly heated by the intense laser field, similar to that found in laser–solid interactions. We have explored the heating and absorption mechanisms by varying the laser pulse duration, while keeping the pulse energy constant and obtained an optimum pulse duration for x-ray yield, plasma temperature and maximum photon energy.

II. EXPERIMENT

A block diagram of the experimental setup is given in Fig. 1. Experiments reported here have been performed in a vacuum chamber maintained at a background pressure of $\sim 10^{-3}$ Torr during the experiment by a 1000 l/s high throughput turbo-molecular pump. Clusters are produced by injecting high pressure krypton gas into the vacuum at 10 Hz through a pulsed cylindrical nozzle. The maximum operating backing pressure is up to 90 bar for the pulsed valve, which has an exit throat diameter of 1 mm. The cylindrical nozzle coupled to the valve exit has a throat of diameter 2 mm and length 15 mm. While an accurate estimate of the cluster size and distribution is difficult,[22,23] a realistic estimate is obtained from the scaling laws established by Hagena.[24] The semiempirical (Hagena) parameter determining the average
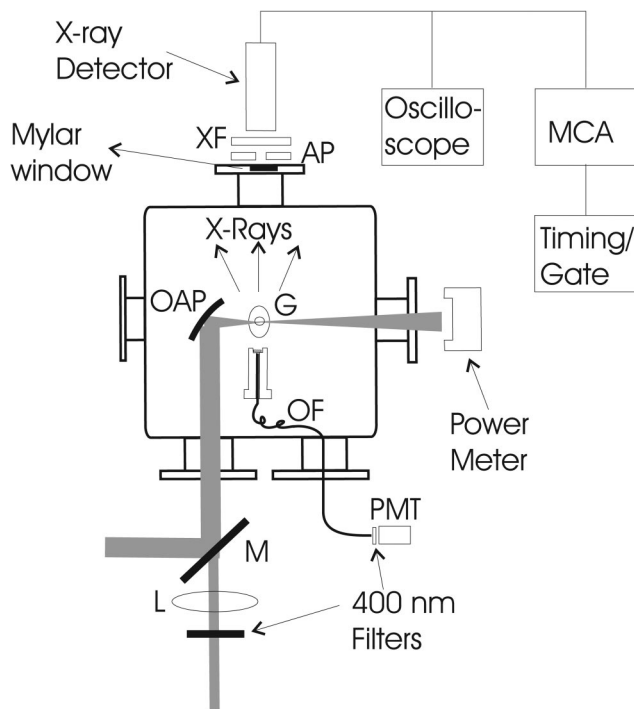
a)Electronic address: riju@strath.ac.uk

FIG. 1. Schematic of the experimental setup. L-lens; M-dielectric turning mirror for 800 nm radiation; OAP-off axis parabola; G-gas jet; OF-optical fibre; PMT-photomultiplier tube; XF-x ray filter; AP-aperture; MCA-multichannel analyzer.

cluster size for an axi-symmetric cylindrical nozzle is $\Gamma^* = k d^{0.85} p_0 / T_0^{2.29}$,[24,25] where d is the nozzle throat diameter in micrometers, p_0 the backing pressure in millibar, T_0 the initial gas temperature in K, and k ($=2890$ for Kr), a constant that depends on the sublimation enthalpy per atom and van der Waals bond length. The cluster size scales as $\langle N \rangle = 33(\Gamma^*/1000)^{2.35}$ for $\Gamma^* > 1000$,[24] which gives an estimate of the mean number of atoms per cluster of between 9.6×10^3 and 1.7×10^6 (average cluster radii, $R_c \sim r_w \langle N \rangle^{1/3} \sim 5$ to 30 nm, where $r_w = 2.57$ Å for Kr) for a backing pressure of between 3 and 30 bar at $T_0 = 293$ K. Rayleigh scattering of a frequency doubled (400 nm) Ti:S laser beam has been used to verify the formation of clusters. In order to measure the scattered signal, a multi-mode pick-off optical fibre is placed very close to the gas jet at 90° to the propagating laser beam. The off-axis parabola shown in Fig. 1 is replaced by a flat reflecting mirror and the low energy 400 nm beam (pulse energy is a few hundred microjoules) is loosely focused on to the gas jet by a long focal length lens as shown in Fig. 1. The scattered signal is measured using a photomultiplier tube after filtering residual 800 nm radiation with band pass filters. The scattered signal scales roughly with the cube of the backing pressure, as expected,[4] when clusters are formed in the jet. Observation of the scattering in only one direction precludes its use to directly characterize the cluster size distribution.

The intense laser excitation is provided by an 800 nm, 60 fs CPA Ti:sapphire laser with maximum pulse power of 5 TW available on the target. The laser is focused into the cluster cloud using a 100 mm focal length UV-grade fused silica lens for pulse energies up to ~ 17 mJ, or an off-axis

parabolic mirror for pulse energies up to 125 mJ. The small B-integral of the UV-grade fused silica lens allows it to be used for pulse energies up to 20 mJ. However, for higher pulse energies nonlinear effects are found to broaden the pulse and hence off-axis parabolas are used. The focal spot size is directly monitored using an imaging beam profiler and the measured beam spot diameter is 16 μm. By translating one of the gratings in the CPA compressor, it has been possible to generate chirped pulses of durations ranging from 60 fs to 2.2 ps. The laser used in the experiments has a nearly Gaussian-type spectral profile centered at 800 nm. Thus we expect the intensity to follow a $1/\tau_p$ scaling, where τ_p is the laser pulse width. The laser interacts with the clustered medium 2 mm above the gas jet nozzle over a length of ~ 3.5 mm. Single photon counting methods using conventional solid state Si:PIN and cadmium zinc telluride (CZT) detectors have been used to measure x-ray spectra in the spectral range 1–50 keV. The Si:PIN detector is very sensitive in the range 1–30 keV and has a measured energy resolution of 250 eV at 6.4 keV. The CZT detector is sensitive over the range 3–90 keV and has a measured energy resolution of 400 eV at 14.4 keV. Single x-ray events are accumulated using a multichannel analyzer, which has been calibrated using a Co^{57} x-ray source. In order to avoid pile up on the accumulated spectrum,[26] average count rates are maintained below 0.1/pulse by a 300 μm diameter aperture and aluminum filters outside the vacuum chamber. X-ray photons are measured at 90° to the laser propagation direction, as shown in Fig. 1. Laser energy transmitted through the cluster jet is measured to estimate the total radiation absorbed by the clusters, since the integrated scattering loss has been shown to be negligible when compared with absorption.[27]

III. RESULTS AND DISCUSSION

Laser absorption in clusters is strongly coupled to their expansion and therefore the pulse duration and intensity play a major role in plasma heating. To investigate this, we have varied the laser pulse duration and measured laser absorption, x-ray spectra, and electron temperature (T_e). Figures 2(a) and 2(b) show typical measured x-ray spectra originating from ~ 18 nm radii Kr clusters with excitation pulse durations of 90 and 300 fs, respectively, and corresponding intensities of 8.8×10^{16} Wcm^{-2} and 2.6×10^{16} Wcm^{-2}, respectively. The spectra are composed of the $K\alpha$ line from krypton superposed on a broad continuum. To ensure that the high energy electrons scattered from the steel vacuum chamber material do not contribute to the continuum spectrum, we have searched for a contribution from k-shell emission from iron at 6.4 keV. The absence of any measurable Fe $K\alpha$ emission discounts the possibility that the background x-ray spectrum includes contributions from high energy electrons scattering off the chamber walls. This is consistent with earlier studies using the setup with low-Z targets such as argon for producing x rays, which also show no evidence of 6.4 keV photons from the steel chamber.

The spectral shape of x rays radiated from Kr clusters, has an exponential dependance at lower energies in addition
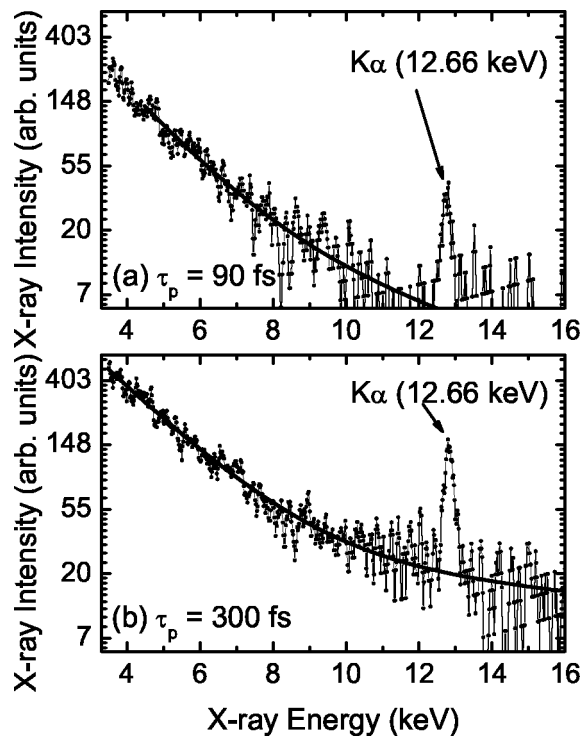
FIG. 2. X-ray spectra from $R_c \sim 18$ nm krypton clusters in the energy range 3.5–16 keV for two different pulse durations (a) 90 fs and (b) 300 fs. Spectra are corrected for filter transmission factors.
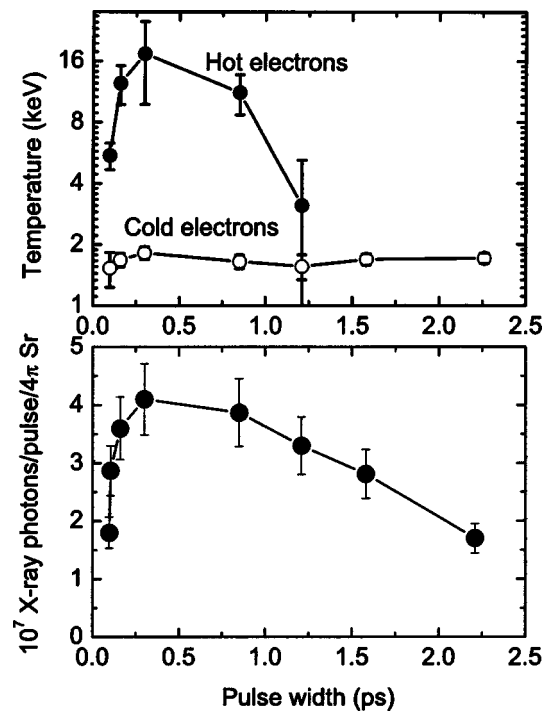

FIG. 3. Dependence of electron temperature corresponding to the two electron components and x-ray yield as a function of laser pulse duration for $R_c \sim 18$ nm.

to a broader tail at higher energies, which is similar to that observed from laser heated solid targets for comparable laser parameters.[2] In a high temperature plasma, inner shell excitation, which is responsible for k-shell emission is due to inelastic electron–ion collisions, and is appreciable only when the electron energy is comparable or exceeds the ionization energy. Thus, observation of the Kα line is evidence of electrons with energies higher than the ionization energy for krypton k-shell electrons (14.3 keV). The integrated x-ray yield exceeds 10^7 photons/pulse/4πSr in the energy range 3.5–16 keV. The measured total x-ray yield is significantly higher than that previously observed for krypton clusters of comparable dimension, and for ~ 20 times higher laser intensity.[16] The highest x-ray energy from krypton observed by Dobosz *et al.*[16] was 1.75 keV, without any evidence of k-shell emission or continuum.

The plasma temperature is estimated from the continuum part of the spectra,[28] which originates from either free-free or free-bound transitions during the interactions of electrons with ions. In both cases, for Maxwellian electron distributions, the spectral intensity depends on the photon energy as, $I(h\nu) \propto \exp(-h\nu/kT_e)$, where h is Planck's constant, and k Boltzmann's constant. In the present case, the measured x-ray intensity is well described by a double exponential function $I_{x-ray} = A_1 \exp(-h\nu/kT_1) + A_2 \exp(-h\nu/kT_2)$, corresponding to a two-temperature electron distribution. Thick solid lines in Fig. 2 are numerical fits to the measured spectra for x-ray photon energies above 3.5 keV. From the double exponential we find that the relative contribution $A_2 T_2/(A_1 T_1 + A_2 T_2)$ of the hot electron fraction to the integrated total x-ray intensity is approximately 10% for all

pulse lengths and relatively constant even though the maximum attained electron temperatures varies with pulse duration.

Figure 3(a) shows the dependance of the two-component electron temperature, which corresponds to the two electron distributions measured as a function of laser pulse duration while keeping the energy density constant at 8 kJcm^{-2}. A maximum electron temperature of 17.6 ± 7.0 keV has been obtained for a pulse duration of 300 fs. The cold electron temperature remains approximately constant at $T_e \sim 1.8 \pm 0.13$ keV for the range of pulse widths examined. X-ray yield from 3 to 15 keV measured a function of pulse duration ($R_c \sim 18$ nm) is shown in Fig. 3(b). An optimum pulse duration exists for maximum x-ray yield. The integrated x-ray yield for fixed cluster size and pulse energy, initially increases significantly with increasing pulse duration until a maximum at 300 fs after which it decreases for much longer pulses. At the highest intensities of the shortest laser pulse duration (60 fs), the yield is a factor 2.5 smaller than that observed at the optimum pulse duration (300 fs).

We have increased the laser intensity for a pulse duration fixed at 60 fs, and did not observe dramatic increase in the temperature of the plasma, even though the x-ray yield grows nonlinearly with intensity.[16] For a laser intensity of 1.3×10^{18} W cm^{-2}, the continuum extends to 45 keV, as shown in Fig. 4. An 800 μm thick aluminum filter, which transmits $\sim 7\%$ at 12.66 keV, and apertures have been used to reduce the x-ray flux on the detector for these measurements. Since thick x-ray filters have been used, the spectrum below ~ 10 keV is not measurable. At these higher excitation intensities it is possible that MeV electrons are being generated.[29] However, due to the reduced collisional cross
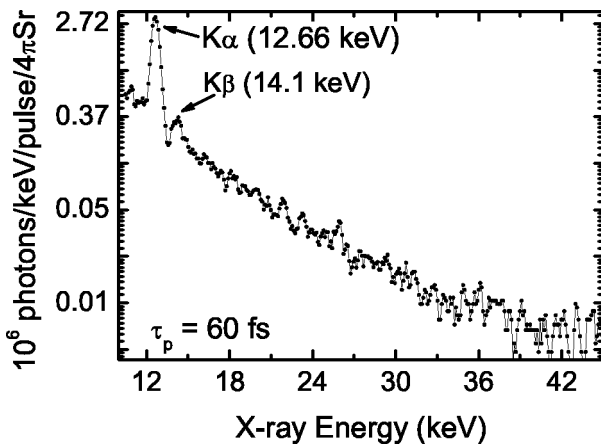
FIG. 4. Hard x-ray spectrum from $R \sim 30$ nm krypton clusters measured for a laser intensity of 1.3×10^{18} Wcm^2 and a pulse duration of 60 fs. The measured electron temperature is 7.6 ± 0.2 keV.

section of these higher energy electrons and the finite cluster volume, it is reasonable to expect that the thermalized electron temperature (as measured through collisions) will be significantly lower. In our measurements the electron temperature is estimated as $\sim 7.6 \pm 0.2$ keV for 1.3×10^{18} Wcm^{-2} from the spectra of Fig. 4, which is roughly equal to the measured hot electron temperature at 90 fs [shown in Fig. 3(a)] for lower peak intensity (8.8×10^{16} Wcm^{-2}). Taking into account the instrumental resolution, the integrated x-ray yield in the Kα line profile is 2.3×10^7 photons per pulse, which is equivalent to 45 nJ Kα x-ray energy per pulse. This corresponds to a laser to Kα conversion efficiency of 9.2×10^{-7}, for 25% absorption (see Fig. 5) of the input laser radiation. These Kα yields and conversion efficiencies are the highest measured values from high atomic number rare gas clusters to date. This compares with a yield of 1.4 nJ from Kr Lα emission measured at 1.75 keV, estimated from the data from Dobosz *et al.*,[16] at 5×10^{17} Wcm^{-2}.

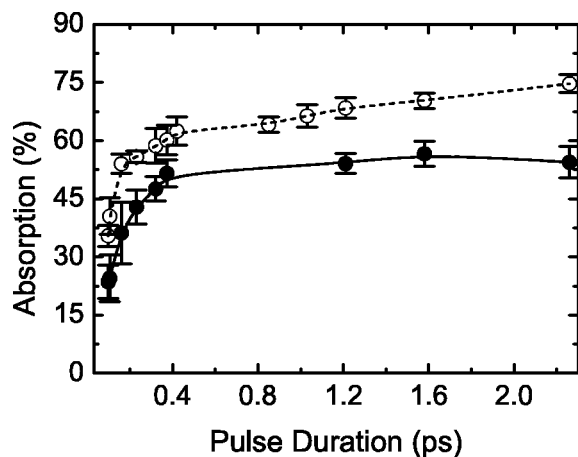Absorption of the laser pulse in the cluster medium has been measured to explore correlations between the tempera-

ture measurements and energy deposition. Figure 5 shows total absorption in the cluster jet measured as a function of laser pulse duration. The absorption for clusters of radii ~ 18 and ~ 30 nm is above 50% for pulses longer than 300 fs, as shown in Fig. 5. For both sizes of clusters, absorption varies weakly with pulse duration above 400 fs. Since the absorption cross section is proportional to R^3, total absorption for a 30 nm cluster should be higher than that for a 18 nm cluster by a factor $(P_1/P_2)^{1.25}(R_2/R_1)^3 \sim 2$, based on the Hagena scaling, where P_1 and P_2 represent backing pressure. According to data shown in Fig. 5, the estimation is a factor of $\sim 1.4 \pm 0.3$ over the range of pulse durations. As shown in Fig. 5, the absorption is less for $\tau_p < 400$ fs irrespective of the cluster size. Published experimental results and calculations based on the nano-plasma model show a similar reduction in absorption for short pulse excitation of Xe clusters of comparable dimensions, and approximately constant absorption up to 2.2 ps.[30] This reduction in total absorption for short duration pulses is ascribed to modifications of the dielectric constant due to the dependence of ν_{ei} on the laser field amplitude. The laser intensity for which the thermal velocity is equal to the oscillation velocity is given by $I[\text{Wm}^{-2}] = 4 \times 10^{-7} \, m_e \omega^2 T_e[\text{eV}]/e$. For intensities higher than this, $v_{os} > v_{th}$, which leads to a decrease in collision frequency.[1,22] Therefore, for $T_e \sim 1.8$ keV and $\lambda = 800$ nm, the oscillation velocity is comparable with the thermal velocity at a laser intensity $\sim 2.6 \times 10^{16}$ Wcm^{-2}, which corresponds to a pulse duration of $\tau_p \sim 300$ fs. Intensity dependant absorption reported elsewhere also shows similar reduction in absorption at high laser intensities.[27]

A number of theoretical models have been proposed to describe the mechanisms of ionization,[31,32] heating,[4,33,34] Coulomb explosion,[35,36] and self-focusing in clustered media.[14] Among these, the nano-plasma model,[4] though generally considered as simplified, has been very successful in explaining laser–cluster interaction and heating. It suggests that the dynamics of the cluster explosion is governed by the time in the laser pulse at which electron density in the cluster passes through Mie resonance, where the electron heating rate is dramatically modified. This explains the existence of an optimum cluster size for a given pulse length.[30] Our calculations presented here are based on the nano-plasma model in which the heating rate is given by[4] $\partial U/\partial t = [\omega/(8\pi)]\text{Im}(\epsilon)|E|^2$, where ϵ_0 is the permittivity of free space, ω the laser frequency, ϵ is the dielectric constant given by[11] $\epsilon(\omega) = 1 - \omega_p^2/[\omega(\omega + i\nu_{ei})]$ with ν_{ei} as the collision frequency, ω_p the plasma frequency and $E = 3E_0/|\epsilon + 2|$, the electric field of the laser inside the cluster, where E_0 is the electric field of the laser in vacuum. The collision frequency is given by $\nu_{ei} \simeq 3 \times 10^{-6} Z n_e T_e[\text{eV}]^{-3/2} \ln \Lambda$, where Z is the average ion charge (taken as 10 in our calculations), $n_e[\text{cm}^{-3}]$ is the electron number density, and $\ln \Lambda$ is the Coulomb logarithm, $\Lambda = 4.9 \times 10^{23} T_e[\text{eV}]^{3/2}/n_e^{1/2}$. However, at high laser intensity the collision frequency decreases and therefore in our model we use an effective collision frequency given by,[1,22] $\nu_{\text{eff}} = \nu_{ei} v_{\text{th}}^3/(v_{\text{osc}}^2 + v_{\text{th}}^2)^{3/2}$, where $v_{\text{th}} = \sqrt{T_e/m_e}$ is the thermal velocity and $v_{\text{osc}} = eE/m_e\omega^2$ is the electron oscillation velocity. Here m_e and e are the electron mass and charge respectively. The inclusion of a field-

FIG. 5. Figure showing absorption of laser radiation measured as a function of pulse duration for two krypton cluster radii, ~ 18 nm (●) and ~ 30 nm (○).

dependant effective collision frequency makes the present calculations distinct from the nano-plasma model formulated by Ditmire et al.[4] The scaling law for the effective collision frequency is normally used in solid density plasmas formed by intense lasers,[1,22] and the similarities between x-ray spectra recorded from clusters and solids provide additional justification for its adoption. Moreover, the above expression for ν_{eff} guarantees a smooth transition between the two limiting cases of laser-cluster interaction, $v_{osc} \ll v_{th}$ and $v_{osc} \gg v_{th}$. Following Ditmire et al.[4] an upper limit for the collision frequency is taken as $\nu_{max} \simeq 2\epsilon E n_i^{1/3}/\pi m_e \omega$, which corresponds to the minimum time it would take an electron driven by the laser field to traverse the distance between two ions. Incorporating this upper limit for the collision frequency, the collision rate is obtained from, $1/\nu = 1/\nu_{eff} + 1/\nu_{max}$. The electric field inside the cluster, $E = 3E_0/|\epsilon + 2|$ is resonantly enhanced to a large value when $\omega = \omega_p/3$. The classical absorption cross section of a single cluster under the dipole approximation and taking into account the small size of clusters compared with the laser wavelength is $\sigma_a = 4\pi(\omega R_c^3/c)\text{Im}[(\epsilon - 1)/(\epsilon + 2)]^{[11]}$ where R_c is the radius of cluster, and c is the speed of light.

After the cluster is ionized, the expansion is driven either by hydrodynamic pressure, or by Coulomb pressure arising from the repulsion between ions. The hydrodynamic pressure, P_H, from hot electrons is $P_H = n_e k T_e$ and the Coulomb pressure is $P_C = Q^2 e^2/(8\pi r^4)$ for a cluster of radius r and charge Qe. The Q/r^4 scaling on the Coulomb pressure indicates its importance for small clusters and for low-Z clusters, where the electrons are not confined and thus Q can become large. Simulations show that P_H dominates over P_C for argon, krypton, and xenon clusters of $r > 2$ nm.[37] Therefore, as a best approximation, hydrodynamic expansion at velocity $v_{exp} = (ZT_e(eV)e/M_i)^{1/2}$, where M_i is the ion mass, determines the rate of change in cluster radius and density in our calculations. Due to relatively long interaction lengths, our calculations includes laser propagation and attenuation according to the Beer–Lambert law. We self-consistently compute the electron energy distribution over the whole interaction volume while taking into account cooling of the plasma due to expansion. The calculations predict an electron temperature in the interaction volume ranging from approximately 100 to 2 keV with a smooth spatial and temporal gradient. The simulations also give a constant plasma temperature for the range of pulse durations in Fig. 3(a). This is consistent with the low temperature component measured in our experiments. However, our calculations do not predict the existence of the hot electron component, which might require inclusions of processes such as avalanche ionization,[31,32] Coulomb explosion,[35,36] self-focusing,[14] resonant heating above the critical density,[33] surface heating of clusters,[34] and many more,[5] into our model. A single model incorporating all these effects does not yet exist and such a complex calculation is beyond the scope of this article.

It is difficult to predict exact mechanisms behind plasma heating and hot electron generation in a cluster plasma. However, a number of plausible explanations for the presence of hot electrons have been presented recently.[4,10,11,33] According to the nano-plasma model a small fraction of electrons may be heated to suprathermal velocities as the expanding nano-plasma undergoes Mie resonance.[4] Moreover, electrons undergo oscillations in the laser field with amplitude given by $x_{os} = eE_0/m_e\omega_0^2$, where e is the electron charge, E_0 is the peak electric field, m_e is the mass of electron and ω_0 is the laser frequency. Since inverse bremsstrahlung collisions are mostly responsible for energy absorption and heating, it is favorable to restrict electron excursions to within the cluster by controlling the laser intensity. The electron oscillation amplitude in the laser field for 300 fs pulses at 2.6×10^{16} Wcm^{-2} is $x_{os} \sim 14$ nm, which is less than the cluster radius. Therefore, there is significant overlap between the electron and ion clouds to facilitate effective collisional absorption. For the shortest pulses used here, the oscillation amplitude is ~ 24 nm and hence the electron cloud overlap with the ions is reduced during the laser pulse, for $R_c \sim 18$ nm clusters. Moreover the collision frequency scales inversely with laser electric field as $\nu_{ei} = (Zen_e m_e \omega^3 \ln \Lambda)/(4\pi\epsilon_0^2 E_0^3)$,[38] and hence rapidly decreases with increasing laser field amplitude. This reduction in collision frequency in conjunction with the larger oscillation amplitude contributes to lower effective heating and x-ray yield with shorter pulses. We conclude that the efficiency of laser coupling to the cluster nano-plasma can be enhanced by altering the electron dynamics in the laser field, for example, by varying the laser pulse width. For pulse durations longer than ~ 300 fs the majority of electrons remain within the cluster enabling better overlap between electron and ion clouds. The constant absorption shown in Fig. 5 measured as a function of pulse length can be due to this restricted electron excursions and subsequent collisional heating. Thus the condition $x_{os} < R_c$ seems to have the major effect on generating hot electrons. Further conclusions would require a more detailed theoretical investigation.

In a recent article, Breizman and Arefieve[37] argued that for cluster radius $R_c \ll x_{os}$, a fraction of electrons that cross the cluster boundary can be stochastically heated to very high electron temperatures when they return to the cluster edge on their oscillatory path in the ion potential well. Electrons that are permanently confined inside the cluster remain relatively cold, therefore, creating a two-temperature electron distribution. Shao et al.[39] observed two components in the electron energy spectrum with distinct features peaking at two different energies. Recently Springate et al.[12] have challenged these findings and established that the electron energy constitutes a wide energy spectrum extending up to 5 keV, without the signature of a two component electron distribution. These electrons are ejected predominantly along the direction of polarization for the laser pulse. Kumarappan et al.[11] observed that single electron temperature adequately describes the measured electron temperature for small clusters, however, for larger clusters a two-temperature distribution is necessary. They have also seen that the low-temperature components arises through Mie resonance,[4] whereas the high temperature component is not strongly influenced by the resonance. In both these latter measurements the cluster density is a few orders of magnitude lower than in the experiments reported in this article. For example, estimated cluster density in the experiments of Springate et al.[12]

was $\sim 10^9$ cm^{-3} compared with an estimated cluster density of $\sim 10^{13}$ cm^{-3} in our experiments. With our higher cluster density, mean spacing between clusters is ~ 200 nm and as the neighboring clusters expand and thermalize they will form a dense, extended plasma on a picosecond time scale. Collisions during plasma formation randomize the electron velocity and the contributions from hot electrons[37] may appear as a distinct component in the x-ray emission spectrum.

In conclusion, we have measured x-ray continuum and 12.66 keV line emission from laser heated krypton clusters, which corresponds to the highest x-ray energies observed to date from any rare gas clusters. Electron energy distributions inferred from the bremsstrahlung x-ray spectra are consistent with a two component plasma with two distinct temperatures. An optimum pulse duration has been found for x-ray yield. Calculations based on the nano-plasma model explain the low temperature component, but not the high temperature component. With the increased yield we observed here such cluster targets may turn out to be a potentially useful debris free, hard x-ray source.

ACKNOWLEDGMENTS

[1] P. Gibbon and E. Forster, Plasma Phys. Controlled Fusion **38**, 769 (1996).
[2] D. Giulietti and L. A. Gizzi, Riv. Nuovo Cimento **21**, 1 (1998).
[3] A. Mc.Pherson, T. S. Luk, B. D. Thompson, A. B. Borisov, O. B. Shiryaev, X. Chen, K. Boyer, and C. K. Rhodes, Phys. Rev. Lett. **72**, 1810 (1994).
[4] T. Ditmire, T. Donnelly, A. M. Rubenchik, R. W. Falcone, and M. D. Perry, Phys. Rev. A **53**, 3379 (1996).
[5] V. P. Krainov and M. B. Smirnov, Phys. Rep. **370**, 237 (2002).
[6] G. C. Junkel-Vives, J. Abdallah, Jr., F. Blasco, C. Stenz, F. Salin, A. Y. Faenov, A. I. Magunov, T. A. Pikuz, and I. Y. Skobelev, Phys. Rev. A **64**, 021201 (2001).
[7] E. Parra, I. Alexeev, J. Fan, K. Y. Kim, S. J. McNaught, and H. M. Milchberg, Phys. Rev. E **62**, 5931 (2000).
[8] S. Ter-Avetisyan, M. Schnurer, H. Stiel, U. Vogt, W. Radloff, W. Karpov, W. Sandner, and P. V. Nickles, Phys. Rev. E **64**, 036404 (2001).
[9] S. Dobosz, M. Schmidt, M. Perdrix, P. Meynadier, O. Gobert, D. Norm, K. Ellert, A. Y. Faenov, A. I. Magunov, T. A. Pikuz *et al.*, J. Exp. Theor. Phys. **88**, 1122 (1999).
[10] L. M. Chen, J. J. Park, K. H. Hong, J. L. Kim, J. Zhang, and C. H. Nam, Phys. Rev. E **66**, 025402 (2002).
[11] V. Kumarappan, M. Krishnamurthy, and D. Mathur, Phys. Rev. A **67**, 043204 (2003).
[12] E. Springate, S. A. Aseyev, S. Zamith, and M. J. J. Vrakking, Phys. Rev. A **68**, 053201 (2003).

[13] T. Ditmire, J. Zweiback, V. P. Yanovsky, T. E. Cowan, G. Hays, and K. B. Wharton, Nature (London) **398**, 489 (1999).
[14] I. Alexeev, T. M. Antonsen, K. Y. Kim, and H. M. Milchberg, Phys. Rev. Lett. **90**, 103402 (2003).
[15] M. J. Edwards, A. J. MacKinnon, J. Zweiback, K. Shigemori, D. Ryutov, R. M. Rubenchik, K. A. Keilty, E. Liang, B. A. Remington, and T. Ditmire, Phys. Rev. Lett. **87**, 085004 (2001).
[16] S. Dobosz, M. Lezius, M. Schmidt, P. Meynadier, M. Perdrix, and D. Normand, Phys. Rev. A **56**, R2526 (1997).
[17] T. Ditmire, T. Donnelly, R. W. Falcone, and M. D. Perry, Phys. Rev. Lett. **75**, 3122 (1995).
[18] Y. Fukuda, K. Yamakawa, Y. Akahane, M. Aoyama, N. Inoue, H. Ueda, and Y. Kishimoto, Phys. Rev. A **67**, 061201 (2003).
[19] W. A. Schroeder, F. G. Omenetto, A. Borisov, J. W. Longworth, A. McPherson, C. Jordan, K. Boyer, K. Kondo, and C. K. Rhodes, J. Phys. B **31**, 5031 (1998).
[20] V. Kumarappan, M. Krishnamurthy, D. Mathur, and L. C. Tribedi, Phys. Rev. A **63**, 023203 (2001).
[21] T. Auguste, P. D'Oliveira, S. Hulin, P. Mono, J. Abdallah, Jr., A. Y. Faenov, I. Y. Skobelev, A. I. Magunov, and T. A. Pikuz, JETP Lett. **72**, 38 (2000).
[22] K. Y. Kim, V. Kumarappan, and H. M. Milchberg, Appl. Phys. Lett. **83**, 3210 (2003).
[23] F. Blasco, T. Caillaud, F. Dorchies, C. Stenz, J. Stevefelt, A. S. Bpldarev, and V. A. Gasilov, Nucl. Instrum. Methods Phys. Res. B **205**, 324 (2003).
[24] O. F. Hagena, Rev. Sci. Instrum. **63**, 2374 (1992).
[25] J. Wormer, V. Guzielski, J. Stapelfeldt, and T. Moller, Chem. Phys. Lett. **19**, 321 (1989).
[26] L. C. Tribedi and P. N. Tandon, Nucl. Instrum. Methods Phys. Res. B **69**, 178 (1992).
[27] T. Ditmire, R. A. Smith, J. W. G. Tisch, and M. H. R. Hutchinson, Phys. Rev. Lett. **78**, 3121 (1997).
[28] B. Yaakobi, F. J. Marshall, and R. Epstein, Phys. Rev. E **54**, 5848 (1996).
[29] X. F. Wang, N. Saleh, M. Krishnan, H. W. Wang, S. Backus, M. Muranane, H. Kapteyn, D. Umstadter, Q. D. Wang, and B. F. Shen, J. Opt. Soc. Am. B **20**, 132 (2003).
[30] J. Zweiback, T. Ditmire, and M. D. Perry, Phys. Rev. A **59**, R3166 (1999).
[31] C. Rose-Petruck, K. J. Schafer, K. R. Wilson, and C. P. J. Barty, Phys. Rev. A **55**, 1182 (1997).
[32] M. Rusek, H. Lagadec, and T. Blenski, Phys. Rev. A **63**, 013203 (2000).
[33] H. M. Milchberg, S. J. McNaught, and E. Parra, Phys. Rev. E **64**, 056402 (2001).
[34] M. B. Smirnov and V. P. Krainov, Phys. Plasmas **10**, 443 (2003).
[35] M. Lezius, S. Dobosz, D. Normand, and M. Schmidt, Phys. Rev. Lett. **80**, 261 (1998).
[36] D. A. Card, E. S. Wisniewski, D. E. Folmer, and J. A. W. Castleman, J. Chem. Phys. **116**, 3554 (2002).
[37] J. W. G. Tisch, N. Hay, K. J. Mendham, E. Springate, D. R. Symes, A. J. Comley, M. B. Mason, E. T. Gumbrell, T. Ditmire, R. A. Smith *et al.*, Nucl. Instrum. Methods Phys. Res. B **205**, 310 (2003).
[38] V. P. Silin, Sov. Phys. JETP **20**, 1510 (1965).
[39] Y. L. Shao, T. Ditmire, J. W. G. Tisch, E. Springate, J. P. Marangos, and M. H. R. Hutchinson, Phys. Rev. Lett. **77**, 3343 (1996).